Journal of Statistical Physics, Vol. 96, Nos. 1/2, 1999

Stochastic One-Dimensional Lorentz Gas on a Lattice

E. Barkai[1] and V. Fleurov[1]

Received August 14, 1998; final February 26, 1999

We study a one-dimensional stochastic Lorentz gas where a light particle moves in a fixed array of nonidentical random scatterers arranged in a lattice. Each scatterer is characterized by a random transmission/reflection coefficient. We consider the case when the transmission coefficients of the scatterers are independent identically distributed random variables. A symbolic program is presented which generates the exact velocity autocorrelation function (VACF) in terms of the moments of the transmission coefficients. The VACF is found for different types of disorder for times up to 20 collision times. We then consider a specific type of disorder: a two-state Lorentz gas in which two types of scatterers are arranged randomly in a lattice. Then a lattice point is occupied by a scatterer whose transmission coefficient is η with probability p or $\eta+\varepsilon$ with probability $1-p$. A perturbation expansion with respect to ε is derived. The ε^2 term in this expansion shows that the VACF oscillates with time, the period of oscillation being twice the time of flight from one scatterer to its nearest neighbor. The coarse-grained VACF decays for long times like $t^{-3/2}$, which is similar to the decay of the VACF of the random Lorentz gas with a single type of scatterer. The perturbation results and the exact ones (found up to 20 collision times) show good agreement.

KEY WORDS: Lorentz gas; random walks; disorder; Mathematica; symbolic programming; velocity autocorrelation function; power law decay.

I. INTRODUCTION

In the deterministic Lorentz gas model a light particle moves between fixed scatterers placed in a d-dimensional space. This model is widely used when investigating diffusion phenomena. When identical spherical scatterers are

[1] School of Physics and Astronomy, Tel-Aviv University, Ramat-Aviv, Tel-Aviv 69978, Israel; e-mail: barkai@mit.edu.

0022-4715/99/0700-0325$16.00/0

distributed randomly in space and at low densities the velocity autocorrelation function (VACF) of the light particle decays according to the power law

$$\langle \mathbf{v}(t)\, \mathbf{v}(0) \rangle \sim t^{-(d/2+1)} \tag{1.1}$$

This well known result and other long tailed memory effects related to the Lorentz gas, have been investigated for nearly three decades.[1–12]

In the stochastic Lorentz gas the deterministic scattering law is replaced by a stochastic one. In this model the light particle can be either transmitted or reflected by a scatterer according to a simple probability law. Grassberger[13] using perturbative and numerical analysis and van Beijeren and Spohn[3, 14] using rigorous methods considered the stochastic one-dimensional Lorentz gas with identical scatterers distributed randomly on a line. This type of disorder will be called here space disorder. A theorem of van Beijeren and Spohn[14] states that the VACF decays not faster then $t^{-3/2}$. It is important to remember that when the collisions are strong (e.g., the transmission coefficient is 1/2), the 3/2 behavior was anticipated already after fifteen or so mean collision times.[13, 14]

The van Beijeren–Spohn theorem[14] does not exclude the possibility of oscillations. Olesky,[15] using numerical simulations, has observed an oscillating VACF for a lattice version of this model. Then fast oscillations found are due to the lattice structure and similar odd/even oscillations were observed in numerical simulation of a stochastic Lorentz gas on a square lattice by Binder and Frenkel.[16]

Lattice Lorentz gases are investigated[15–22] mainly due to their simplicity and because they capture some of the essential features of non lattice gases. Ernst *et al.*[23, 24] have investigated a one-dimensional Lorentz gas with one type of scatterers distributed randomly on a lattice within mean field theory approach. Using a dynamical partition function they have estimated the chaotic dynamical properties of the system, such as Lyaponov exponent and Kolmogorov–Sinai entropy. This venue of research is of a particular interest since it relates between chaotic dynamical properties and the transport coefficients, an issue developed by Gaspard and Nicolis.[7]

In Section II we give definitions and working tools with which a one-dimensional stochastic Lorentz gas is studied. In this model scatterers are arranged randomly on a lattice. The scatterer on site m is characterized by its transmission coefficient T_m which is a random variable. Differently from the previous works we do not assume that the lattice points are either occupied or unoccupied, rather we consider the case when the T_m's are distributed randomly in the interval (0, 1). Throughout the motion of the light particle its kinetic energy is conserved and the disorder is static.

For lattice Lorentz models one can find exact solutions by counting trajectories and giving them the proper statistical weight. This is a cumbersome task which can be carried out only for very short times. In Section III we use the symbolic powers of Mathematica[25] to solve the model exactly and find the VACF, the only assumption on the disorder is that the scatterers transmission coefficients are independent identically distributed random variables. The main limitation on such an exact approach is the machine computation time and finite memory. We find the VACF for the case when the light particle has encountered up to twenty collisions. When collisions are strong, twenty collisions are sufficient to reduce the VACF by a few orders of magnitude from its initial value. Our solution is then used to investigate the behavior of the VACF for different types of disorder. It might be a useful tool with which approximate solutions, found using either analytical or numerical methods could be checked. In certain cases our exact result can be used to find how long one has to wait until the asymptotic behavior of the VACF is first observed.

In Section IV we investigate in greater detail the case where two types of scatterers are arranged on the underlying lattice. This corresponds to a random $A-B$ alloy where sites are not equivalent. We call this type of model the two state Lorentz gas (TSLG). With a probability p a lattice point is occupied by a scatterer whose transmission coefficient is η and with probability $1-p$ it is occupied by a scatterer whose transmission coefficient is $\eta+\varepsilon$. We develop an ε perturbation expansion. The lowest order term in our expansion describes an ordered system with an effective transmission coefficient $T=\eta+\varepsilon(1-p)$ and reflection coefficient $R=1-T$ associated with each scatterer on the lattice. For this ordered case the VACF decays exponentially with a rate constant which can become complex. The ε^2 correction shows that the VACF oscillates, the period being twice the time of flight from one scattering center to its nearest neighbor. The amplitude of these oscillations decays as $t^{-3/2}$; which is characteristic of the VACF decay of a particle exhibiting Gaussian diffusion in quenched environment in one-dimension. The exact and perturbative solutions are compared and we find a good agreement between the two for times shorter than twenty collision times.

II. STOCHASTIC ONE DIMENSIONAL LORENTZ GAS

For the stochastic one dimensional Lorentz gas a light particle runs with a constant speed $v>0$, and makes instantaneous collisions with scatterers. We shall consider the case where the scatterers are arranged on lattice with a lattice constant a (random walks on lattices are discussed in ref. 26). The lattice sites are numbered ($m=0, 1,..., M-1$) and periodic

boundary conditions are assumed. The probability of transmission at a lattice point m is T_m and the reflection probability is $R_m = 1 - T_m$.

Let $P_m^+(t)[P_m^-(t)]$ be the probability of finding at time t the light particle with a velocity v $[-v]$, on site m. The time $\tau = a/v$ is the time it takes the light particle to move from one lattice point to one of its two nearest neighbors. We use the normalized initial condition

$$\sum_m [P_m^+(0) + P_m^-(0)] = 1 \tag{2.1}$$

which means that we exclude the possibility of finding the light particle at time $t = 0$ in the intervals between the scatterers. Only when $t = n\tau$, $(n = 0, 1, 2,...)$, may $P_m^{\pm}(t)$ get values different from zero. Below we shall use $\tau = 1$ meaning that $t = n$. The periodic boundary condition $P_{m+M}^{\pm}(n) = P_m^{\pm}(n)$ are applied.

The recursion relations for the stochastic Lorentz gas on a lattice are

$$\begin{aligned} P_m^+(n+1) &= T_m P_{m-1}^+(n) + R_m P_{m+1}^-(n) \\ P_m^-(n+1) &= R_m P_{m-1}^+(n) + T_m P_{m+1}^-(n) \end{aligned} \tag{2.2}$$

The stationary solution of Eq. (2.2) satisfying $P_m^{\pm}(n+1) = P_m^{\pm}(n)$ is $P_m^{\pm}(n) = C$, with $C = 1/(2M)$ being a constant independent of the T_m values. This constant is determined from the normalization condition

$$\sum_m [P_m^+(n) + P_m^-(n)] = 1$$

We recall that the properties of the discrete Fourier–Laplace transforms[27] are well suited to deal with discrete space-time systems like in the problem we consider here. Therefore we shall use the following mathematical tools:

(a) The Fourier transform of $P_m^{\pm}(n)$ is

$$P_q^{\pm}(n) = \sum_{m=0}^{M-1} e^{iqm} P_m^{\pm}(n) \tag{2.3}$$

where $q = (2\pi l/M)$ lies in the first Brilloin zone (1BZ), namely $l = -\frac{1}{2}M + 1,..., \frac{1}{2}M$.

(b) The orthogonality relations read

$$M^{-1} \sum_{m=0}^{M-1} e^{im(q-q')} = \delta_{qq'} \tag{2.4}$$

and

$$M^{-1} \sum_{q=1BZ} e^{iq(j-m)} = \delta_{jm} \tag{2.5}$$

(c) The discrete Fourier–Laplace transform of $P_m^{\pm}(n)$ is defined as

$$\hat{P}_q^{\pm}(z) = \sum_{n=0}^{\infty} P_q^{\pm}(n)\, z^{-n} \tag{2.6}$$

(d) The inverse discrete Laplace transform, also called[27] the inverse z transform, reads

$$P_q^{\pm}(n) = \frac{1}{2\pi i} \oint \hat{P}_q^{\pm}(z)\, z^{n-1}\, dz \tag{2.7}$$

where the integration is carried out along a closed contour which encloses all the singularities of $\hat{P}_q^{\pm}(z)$. Hence-forward the limits of the sums over m and q will be dropped.

We shall now use these mathematical tools to find a formal solution to the problem. Equations (2.2) are Fourier–Laplace transformed,

$$z[\hat{P}_q^{+}(z) - P_q^{+}(0)] = -\sum_{q'} \{L_{qq'}^{++}\, \hat{P}_{q'}^{+}(z) + L_{qq'}^{+-}\, \hat{P}_{q'}^{-}(z)\}$$

and

$$z[\hat{P}_q^{-}(z) - P_q^{-}(0)] = -\sum_{q'} \{L_{qq'}^{-+}\, \hat{P}_{q'}^{+}(z) + L_{qq'}^{--}\, \hat{P}_{q'}^{-}(z)\} \tag{2.8}$$

Here

$$\begin{aligned} L_{qq'}^{++} &= -T_{qq'} e^{iq'}, & L_{qq'}^{+-} &= -R_{qq'} e^{-iq'} \\ L_{qq'}^{--} &= -T_{qq'} e^{-iq'}, & L_{qq'}^{-+} &= -R_{qq'} e^{iq'} \end{aligned} \tag{2.9}$$

and

$$T_{qq'} = \frac{1}{M} \sum_m e^{i(q-q')m} T_m, \qquad R_{qq'} = \frac{1}{M} \sum_m e^{i(q-q')m} R_m \tag{2.10}$$

Equation (2.8) can be written in matrix form as

$$(z + L)\, \hat{P}_q(z) = z P_q(0) \tag{2.11}$$

with

$$\hat{P}_q(z) = \begin{pmatrix} \hat{P}_q^+(z) \\ \hat{P}_q^-(z) \end{pmatrix}, \qquad P_q(0) = \begin{pmatrix} P_q^+(0) \\ P_q^-(0) \end{pmatrix} \tag{2.12}$$

and

$$L = \begin{pmatrix} L^{++} & L^{+-} \\ L^{-+} & L^{--} \end{pmatrix} \tag{2.13}$$

The formal solution of the problem is

$$\langle \hat{P}_q(z) \rangle = \left\langle \frac{z}{z+L} P_q(0) \right\rangle \tag{2.14}$$

where the average $\langle \cdots \rangle$ is over the random variable T_m. The nontrivial task is to invert the matrix $z+L$ and then average over the disorder.

There are techniques, used already in the context of hopping models (solution of master equation) and developed by Zwanzig[28] and later by Denteneer and Ernst,[29] that make under certain conditions the treatment of equations of the type (2.14) possible. This venue will be followed in Section IV. However first we turn to give the exact solution of the problem using the symbolic programming approach.

III. EXACT SOLUTION—A SYMBOLIC PROGRAMMING APPROACH

An exact solution for the Lorentz gas on a lattice for a broad class of disorder can be expressed in terms of a symbolic program. We have used Mathematica[25] to generate the exact solution for the problem for finite times n. The only assumption we use is that the transmission coefficients T_m are independent identically distributed random variables. In Appendix A a symbolic program is given, with which the averaged over disorder VACF

$$\langle v(n)\, v(0) \mid v(0) = +1 \rangle = \sum_m [\langle P_m^+(n) \rangle - \langle P_m^-(n) \rangle] \tag{3.1}$$

is found. The short program first solves the recursion relation Eq. (2.2) for an array of random scatterers on a system of finite length. The VACF is expressed in terms of $P_m^{\pm}(n)$ which depend in turn on $\{T_m\}$. It is then

expanded in a power series depending on the transmission coefficients, a characteristic term in this expansion being

$$C^{i_1,\ldots,i_n}_{m_1,\ldots,m_n}(T_{m_1})^{i_1}\cdots(T_{m_n})^{i_n} \tag{3.2}$$

Here $C^{i_1,\ldots,i_n}_{m_1,\ldots,m_n}$ are constants, the integers $(m_1,\ldots,m_n)$ denoting the location of the scatterers and $(i_1,\ldots,i_n)$ being integers. Averaging over disorder is carried out by the replacement $(T_m)^i \to \langle (T_m)^i \rangle$. Such a replacement is justified since $\{T_m\}$ are independent random variables. Since $\{T_m\}$ are also identically distributed $\langle (T_m)^i \rangle = \langle T^i \rangle$ is independent of the location m. Hence the characteristic term, Eq. (3.2), is replaced by

$$C^{i_1,\ldots,i_n}_{m_1,\ldots,m_n}\langle T^{i_1}\rangle\cdots\langle T^{i_n}\rangle \tag{3.3}$$

In this way the exact solution is found for finite time.

Our program considers the case when the light particle is initially located at the origin, and has a velocity equal to one directed to the right. The maximal distance $l_{\max}$, the light particle may travel during the time n is $l_{\max}=n$, and therefore if we compute the VACF for n time steps we consider a lattice in the interval $(-l_{\max}, l_{\max})$. This means that we do not use the periodic boundary conditions of the previous section, since, the choice of boundary condition is unimportant when considering the system for a finite time so that the particle cannot reach the boundaries.

Our results are shown in Table 1. For the sake of space we give our results only for $n \leqslant 7$. As mentioned, terms for $n \leqslant 20$ were used and with them the examples of the following subsection are worked out. The limitation on the computation of higher order terms is the time of the computation and the finite memory of the computer.

A few expected features can be seen in Table 1. First when $\langle T^i \rangle = 0$, meaning that the system is composed of perfect reflectors, the VACF alternates between the values $+1$ and -1. Then we notice that if $\langle T^i \rangle = 1$ the VACF is equal unity for all times as expected from a transmitting system. If $\langle T^i \rangle = 1/2^i$ then the VACF is equal zero for $n \geqslant 1$ since then the particle has the velocity $+1$ (or -1) with probability $1/2$. The moments in the solution cannot be higher than $\langle T^{n/2} \rangle$ for even n and $\langle T^{(n+1)/2} \rangle$ for odd n.

When n is even, trajectories of particles which encounter $n/2$ collisions with the scatterer situated at $m=1$ are responsible for the terms which depend on $\langle T^{n/2} \rangle$. The $4\langle T^{n/2} \rangle^2$ term is due to trajectories which bounce back and forth between the scatterers at $m=1$ and $m=0$ or between the scatterers at $m=1$ and $m=2$. Since n is even the particle at time n is located at either $m=0$ or $m=2$ and since at this time the particle can get velocity either $+v$ or $-v$ there are four possible such trajectories, which explains the prefactor four.

Table 1

n	$\langle v(n)\, v(0) \mid v(0) = +1 \rangle$
0	1
1	$-1 + 2\langle T\rangle$
2	$1 - 4\langle T\rangle + 4\langle T\rangle^2$
3	$-1 + 6\langle T\rangle - 8\langle T\rangle^2 + 4\langle T^2\rangle - 4\langle T^2\rangle + 4\langle T\rangle\langle T^2\rangle$
4	$1 - 8\langle T\rangle + 16\langle T\rangle^2 - 8\langle T\rangle^3 + 4\langle T\rangle^4 + 8\langle T^2\rangle$ $- 24\langle T\rangle\langle T^2\rangle + 8\langle T\rangle^2\langle T^2\rangle + 4\langle T^2\rangle^2$
5	$-1 + 10\langle T\rangle - 24\langle T\rangle^2 + 20\langle T\rangle^3 - 8\langle T\rangle^4 + 4\langle T\rangle^5$ $- 16\langle T^2\rangle + 52\langle T\rangle\langle T^2\rangle - 40\langle T^2\rangle\langle T^2\rangle$ $+ 8\langle T\rangle^3\langle T^2\rangle - 16\langle T^2\rangle^2 + 12\langle T\rangle\langle T^2\rangle^2 + 8\langle T^3\rangle$ $- 16\langle T\rangle\langle T^3\rangle + 4\langle T\rangle^2\langle T^3\rangle + 4\langle T^2\rangle\langle T^3\rangle$
6	$1 - 12\langle T\rangle + 36\langle T\rangle^2 - 32\langle T\rangle^3 + 24\langle T\rangle^4$ $- 8\langle T\rangle^5 + 4\langle T\rangle^6 + 24\langle T^2\rangle - 112\langle T\rangle\langle T^2\rangle$ $+ 96\langle T\rangle^2\langle T^2\rangle - 48\langle T\rangle^3\langle T^2\rangle + 8\langle T\rangle^4\langle T^2\rangle + 56\langle T^2\rangle^2$ $- 56\langle T\rangle\langle T^2\rangle^2 + 24\langle T\rangle^2\langle T^2\rangle^2$ $- 16\langle T^3\rangle + 64\langle T\rangle\langle T^3\rangle - 40\langle T\rangle^2\langle T^3\rangle - 40\langle T^2\rangle\langle T^3\rangle$ $+ 24\langle T\rangle\langle T^2\rangle\langle T^3\rangle + 4\langle T^3\rangle^2$
7	$-1 + 14\langle T\rangle - 48\langle T\rangle^2 + 56\langle T\rangle^3 - 40\langle T\rangle^4 + 28\langle T\rangle^5 - 8\langle T\rangle^6 + 4\langle T\rangle^7$ $- 36\langle T^2\rangle + 184\langle T\rangle\langle T^2\rangle - 224\langle T\rangle^2\langle T^2\rangle + 120\langle T\rangle^3\langle T^2\rangle$ $- 56\langle T\rangle^4\langle T^2\rangle + 8\langle T\rangle^5\langle T^2\rangle - 120\langle T^2\rangle^2 + 196\langle T\rangle\langle T^2\rangle^2$ $- 96\langle T\rangle^2\langle T^2\rangle^2 + 28\langle T\rangle^3\langle T^2\rangle^2 - 24\langle T^2\rangle^3 + 12\langle T\rangle\langle T^2\rangle^3 + 40\langle T^3\rangle$ $- 160\langle T\rangle\langle T^3\rangle + 140\langle T\rangle^2\langle T^3\rangle - 32\langle T\rangle^3\langle T^3\rangle + 140\langle T^2\rangle\langle T^3\rangle$ $- 160\langle T\rangle\langle T^2\rangle\langle T^3\rangle + 32\langle T\rangle^2\langle T^2\rangle\langle T^3\rangle + 12\langle T^2\rangle^2\langle T^3\rangle$ $- 24\langle T^3\rangle^2 + 16\langle T\rangle\langle T^3\rangle^2$ $- 16\langle T^4\rangle + 48\langle T\rangle\langle T^4\rangle - 24\langle T\rangle^2\langle T^4\rangle - 24\langle T^2\rangle\langle T^4\rangle$ $+ 12\langle T\rangle\langle T^2\rangle\langle T^4\rangle + 4\langle T^3\rangle\langle T^4\rangle$

Calculation by means of Mathematica is not restricted to the VACF. In fact it is easy to generate also the probability functions $\langle P_m^{\pm}(n)\rangle$ as well as other statistical characteristics of the system. Here we concentrate on the VACF which is the main statistical function investigated in this work.

A. Examples

(a) As mentioned in the introduction, the two state Lorentz gas (TSLG) is defined with two types of scatterers: $T_m = \eta$ with probability p, and $T_m = \eta + \varepsilon$ with probability $1 - p$. Then using the identity

$$\langle T^i\rangle = p\eta^i + (1-p)(\eta+\varepsilon)^i \tag{3.4}$$

it is easy to express the VACF presented in Table 1 in terms of ε, p and η. Note that Eq. (3.4) exhibits an exponential decay of $\langle T^i\rangle$ with respect

to i. We shall consider here the case $\varepsilon = 1/25$, $\eta = 12/25$ and $p = 1/2$. Since for this case $\langle T \rangle = 1/2$, then the mean field approach in which the transmission coefficients are replaced by the averaged value (i.e., take $T_m = 1/2$ for all m) will guarantee that the VACF is zero after a single collision. Since both η and $\eta + \varepsilon$ are close to 1/2 the collisions can be considered strong. Note that the term strong collision might be used for the case where $T_m = 0$, however for this case there is no relaxation of the VACF. Indeed as we show in Fig. 1 the VACF decays from its initial condition to small finite values, however not surprisingly, unlike the mean field approach the VACF does not become zero after the first collision. Rather we observe a slow 3/2 power law decay of the VACF (dashed line) with an oscillating amplitude. This behavior will be explained in detail in Section IV.

So far we have considered the case where at time $t = 0$ the particle is situated on a lattice point. A more interesting situation, from a physical point of view, is the case when the light particle is situated randomly on the real line. At $t = 0$ a set of scatterers (black dots) is given schematically by:

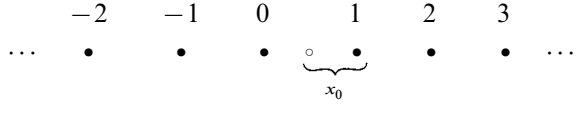

and the light particle (open circle) is situated in the interval $[0, 1]$. The distance x_0 is defined to be the distance between the initial location of the light particle and first scatterer on $m = 1$ (even if $T_1 = 1$). Now the VACF $\langle v(t)\, v(0) \mid v(0) = +1 \rangle_{x_0}$, for continuous time t, depends on the random variable x_0, which is described by a probability density function

$$\mu(x_0) = \begin{cases} 1, & \text{if} \quad x_0 < 1 \\ 0, & \text{otherwise} \end{cases} \tag{3.5}$$

meaning we are considering an equilibrium situation. Averaging the VACF over initial conditions x_0 it is straightforward to show

$$\begin{aligned} &\mathrm{Av}\langle v(t)\, v(0) \mid v(0) = +1 \rangle_{x_0} \\ &\quad = \{1 - [t - \mathrm{Int}(t)]\} \langle v[\mathrm{Int}(t)]\, v(0) \mid v(0) = +1 \rangle \\ &\qquad + [t - \mathrm{Int}(t)] \langle v[\mathrm{Int}(t) + 1]\, v(0) \mid v(0) = +1 \rangle \end{aligned} \tag{3.6}$$

and $\mathrm{Int}(t)$ is the integer part of t. Since we can calculate $\langle v[\mathrm{Int}(t)]\, v(0) \mid v(0) = +1 \rangle$ for $\mathrm{Int}[t] \leqslant 20$ using Mathematica (i.e., Table 1), we can find the VACF Eq. (3.6) for times $0 \leqslant t \leqslant 20$. For a graphic representation of $\mathrm{Av}\langle v(t)\, v(0) \mid v(0) = +1 \rangle_{x_0}$ as a function of time t, we need only to connect

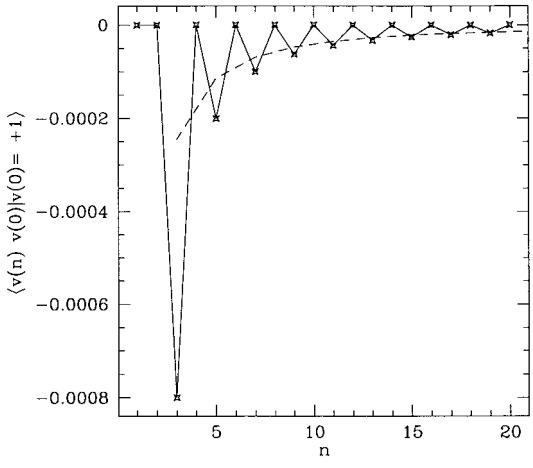

Fig. 1. $\langle v(n)\, v(0) \mid v(0) = +1 \rangle$ vs n for the TSLG model with $\eta = 12/25$, $p = 1/2$ and $\varepsilon = 1/25$. Not shown is the VACF for $n = 0$ which is unity. The dashed line is the asymptotic $n^{-3/2}$ behavior, Eq. (4.44), which is valid only for odd n. For even n the VACF gets a small value which is non-zero. Our program gives exact results with no numerical approximations. For the discrete time n the straight lines are added to guide the eye. They also represent Eq. (3.6), $\mathrm{Av}\langle v(t)\, v(0) \mid v(0) = +1 \rangle_{x_0}$ as a function of the continuous time t.

the discrete points $\langle v(n)\, v(0) \mid v(0) = +1 \rangle$ as done already in Fig. 1 and the figures to follow. Thus the curves in these figures represent the continuous time solution after averaging over the initial location of the light particle using Eq. (3.6), namely they show both the discrete time solutions and $\mathrm{Av}\langle v(t)\, v(0) \mid v(0) = +1 \rangle_{x_0}$ as a function of time t.

(b) The VACF for a uniform probability density function of transmission coefficients is now considered. The moments in this case are given by

$$\langle T^i \rangle = 1/(i+1) \tag{3.7}$$

exhibiting a power law decay with respect to i. The VACF for this case is shown in Fig. 2. After twenty collisions the VACF decays to a value which is roughly 1% of its initial value. It exhibits oscillations, their period being twice the mean collision time. It is interesting to note that the amplitude of these oscillations is not decaying monotonically, therefore a power law decay is not suited to describe the behavior of the VACF, at least for the time window we consider.

We compare the VACF found for the uniform model with the VACF of the TSLG model with $p = 1/2$, $\eta = (6 - 2\sqrt{3})/12$ and $\varepsilon = \sqrt{3}/3$. Such a choice of parameters ensures that for the TSLG model $\langle T \rangle = 1/2$, $\langle T^2 \rangle = 1/3$

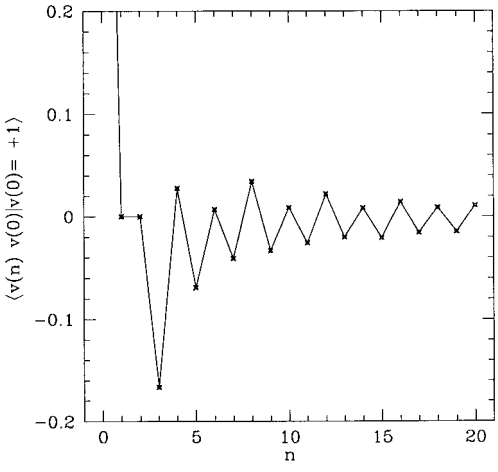

Fig. 2. $\langle v(n)\, v(0) \mid v(0) = +1 \rangle$ vs n for T_m's which are independent identically distributed random variables whose probability density function is uniform in (0, 1). One sees that for n even and $4 \leqslant n \leqslant 20$ the VACF is a non-monotonic function of time. Also when n is odd and $3 \leqslant n \leqslant 19$ the VACF is non-monotonic, since $\langle v(15)\, v(0) \mid v(0) = +1 \rangle < \langle v(13)\, v(0) \mid v(0) = +1 \rangle$.

and $\langle T^3 \rangle = 1/4$. Thus according to Eq. (3.7) for this choice of parameters the first three moments of the T_ms are identical for both distributions. The VACFs for these two types of disorder are given in Table 2 together with the ratio $\langle v(n)\, v(0) \mid v(0) = +1 \rangle_{Uniform} / \langle v(n)\, v(0) \mid v(0) = +1 \rangle_{TSLG}$. We see that for each n the signs of the two VACFs are identical. One can also see that for $n \leqslant 6$ the two VACFs coincide, as can be anticipated, from Table 1. However for $6 < n < 20$ there are large deviations between the two models. We also notice that the ratio is larger or equal to unity, indicating that for the uniform probability density function the VACF decay is slower than the decay of the TSLG VACF. This is probably due to the fact that for $i > 3$ the moments $\langle T^i \rangle$ of the uniform distribution are larger than those of the TSLG model for our special choice of parameters. The difference between the two models, shown in Table 2, implies that the information contained in the first three moments of T_m is not sufficient to determine even approximately the behavior of the VACF.

The relatively slow decay of the VACF of the uniform model raises the question if such a model exhibits normal Gaussian diffusion. It is an open question under what conditions does a one-dimensional stochastic Lorentz gas exhibit an anomalous diffusion with $\langle x^2 \rangle \sim t^\alpha$ and $\alpha \neq 1$. Such an anomalous behavior may be expected to depend on the behavior of the probability density function of the transmission coefficients near $T = 0$.

Table 2

n	$\langle v(n)\, v(0) \mid v(0) = +1 \rangle_{TSLG}$	$\langle v(n)\, v(0) \mid v(0) = +1 \rangle_{Uniform}$	Ratio
0	1	1	1
1	0	0	
2	0	0	
3	−0.166666	−0.166667	1
4	0.027778	0.027778	1
5	−0.069444	−0.069444	1
6	0.006944	0.006944	1
7	−0.024306	−0.040972	1.68567
8	0.021798	0.034267	1.57202
9	−0.019194	−0.033453	1.74289
10	0.006221	0.008659	1.3919
11	−0.009299	−0.025681	2.76169
12	0.008971	0.021906	2.44187
13	−0.00712	−0.020120	2.82584
14	0.003824	0.008292	2.16841
15	−0.006447	−0.020686	3.20862
16	0.004135	0.014191	3.43192
17	−0.004551	−0.015501	3.40606
18	0.003150	0.008904	2.82667
19	−0.003883	−0.014504	3.73526
20	0.002501	0.010750	4.29828

One can quantify this assumption using Scher–Lax–Montroll (SLM) approach[30–33] which has been used extensively to model transport in disordered media. The basic idea is to replace the disordered system by an ordered one, with a suitably chosen waiting time probability density function $\psi(t)$ and then analyze the random walk using the continuous time random walk (CTRW). Using the SLM approach we consider a light particle on $m = 0$ with a velocity $+1$. The particle will escape the length interval $[0, 1]$ once it is transmitted through either the scatterer on $m = 0$ or that on $m = 1$. Consider the paths for which the particle may escape only through $m = 1$. Then the probability the particle did not escape the interval $[0, 1]$ in the time interval $[0, n]$ is $Q(n) = \langle R_1^{n/2} \rangle$ for even n. The CTRW waiting time probability density function is $\psi(n) = (d/dn)\, Q(n)$. Using this function within the CTRW theory we find for the uniform density model $\langle x^2 \rangle \sim n/Ln(n)$. Thus within this CTRW framework the stochastic Lorentz gas with a uniform density of transmission coefficients exhibits a sub diffusive behavior which is different from the normal behavior of the TSLG and space disorder models. An even slower diffusion with $\langle x^2 \rangle \sim n^{\alpha}$ might be expected for Lorentz systems with a probability density function of

reflecting coefficients $f(R)$ behaving like $f(R) = \alpha(1-R)^{-(1-\alpha)}$ and $0 < \alpha < 1$. It is still left to be seen if such an anomalous behavior can be predicted basing upon a rigorous approach.

(c) We now consider space disorder where with probability p a lattice point is occupied by a scatterer with transmission coefficient η, and with probability $(1-p)$ it is vacant (i.e., $T_m = 1$). This is a special case of the TSLG when $\eta + \varepsilon = 1$. Then

$$\langle T^i \rangle = p\eta^i + (1-p). \tag{3.8}$$

Unlike the moments of the uniform distribution Eq. (3.7) and the moments of the TSLG model Eq. (3.4) (i.e., when $\eta + \varepsilon \neq 1$), here we are dealing with the situation where $\lim_{i \to \infty} \langle T^i \rangle = (1-p)$ while for the other two models $\lim_{i \to \infty} \langle T^i \rangle = 0$.

This case is analyzed using the results obtained by van Beijeren and Spohn.[14] Briefly, they have considered the stochastic Lorentz gas with identical scatterers distributed randomly on the real line and examined the case $\eta = 1/2$. In this model time t is continuous. At time $t = 0$ the particle is randomly located on a line among the point scatterers (i.e., not necessarily on a lattice point). Hence averages are over (a) initial condition of the light particle and (b) random realizations of scatterers realizations (i.e., the spatial disorder). van Beijeren and Spohn proved

Theorem. For given β in the range $0 < \beta < 1/2$

$$\mathrm{Av} \left\langle \int_0^\infty \exp(-ut)[\, v(t)\, v(0) \mid v(0) = +1 \,]\, dt \right\rangle_{x_0} = \frac{\langle \xi \rangle^2}{2\tau} + (2u\tau)^{1/2} \frac{\langle \xi^2 \rangle - \langle \xi \rangle^2}{4\tau} + \mathrm{O}((u\tau)^{1-\beta}) \tag{3.9}$$

Here $\langle \xi \rangle$ and $\langle \xi^2 \rangle$ are the first and second moments of the distances between the scatterers. $\tau = \langle \xi \rangle$ is the mean free time between collision events and u is the usual Laplace variable. As mentioned in ref. 14 this bound is too weak to prove an asymptotic power law decay of the VACF. The theorem shows that the VACF decays not faster than $t^{-3/2}$.

Assuming that oscillations vanish when $t \to \infty$ we inverse Laplace transform Eq. (3.9), finding

$$\mathrm{Av} \langle v(t)\, v(0) \mid v(0) = +1 \rangle_{x_0} \simeq -\frac{1}{4\sqrt{2\pi}} \frac{\langle \xi^2 \rangle - \langle \xi \rangle^2}{\tau^{1/2}}\, t^{-3/2} \tag{3.10}$$

This result might be expected to work well for large t and conjectured to be observed after roughly fifteen collision times. We again remind the reader that in ref. 14 the possibility of a superposition of oscillations was not ruled out.

For scatterers on a lattice we have $\langle \xi \rangle = 1/p$ and $\langle \xi^2 \rangle = (2-p)/p^2$ and therefore from Eq. (3.10)

$$\mathrm{Av}\langle v(t)\, v(0) \mid v(0) = +1 \rangle_{x_0} \simeq -\frac{(1-p)}{4\sqrt{2\pi}(pt)^{3/2}} \tag{3.11}$$

Even though we expect to observe oscillations in the long time solution, due to the underlying lattice structure, one may hope that this equation describes well the decay of the amplitude of these oscillations, at least for large times.

The asymptotic result Eq. (3.11) is shown in Fig. 3 together with our exact result obtained using the symbolic programming approach, for the special case $p = 199/200$. This choice of p implies that after 20 time steps the light particle has encountered on the average nearly twenty collisions. We see in Fig. 3 that the VACF exhibits the characteristic oscillations caused by the underlying lattice and found here already for two other

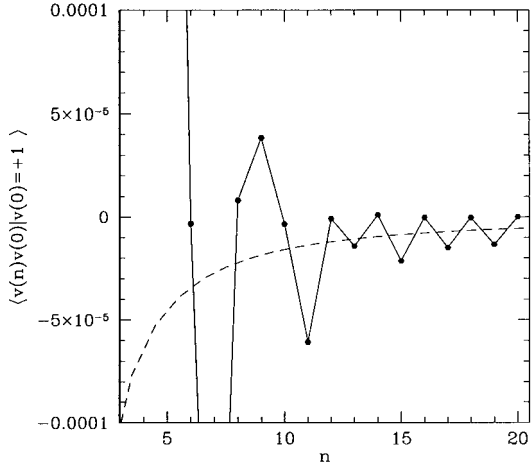

Fig. 3. $\langle v(n)\, v(0) \mid v(0) = +1 \rangle$ vs n for space disorder where with probability 199/200, $T_m = 1/2$ and $T_m = 1$ otherwise. The dashed curve is the $n^{-3/2}$ behavior, Eq. (3.11). Notice that even when the VACF has decayed five orders of magnitude from its initial value it is still not monotonic its values for even n being above the dashed curve while values for even n lying under it. Moreover, each of these values converge (if at all) to the asymptotics very slowly and also not monotonically.

models. One can also see from Fig. 3 that our VACF does not decay faster than the van Beijeren–Spohn bound Eq. (3.11). However one may also conclude that Eq. (3.11) is not a good approximation for the VACF, at least for $n \leqslant 20$. This does not mean that our result contradicts the van Beijeren–Spohn theorem, Eq. (3.9), rather it implies that one cannot use the Laplace $u \to t$ transform Eq. (3.10), to predict the asymptotic behavior of the VACF.

All the examples in this subsection where calculated on the Challenge R10000 Silicon Graphic computer at the computer center at Tel Aviv university (for more details see ref. 34). For $n = 20$ the CPU time was 53300 seconds, the maximum memory was 394 MB and maximum swap was 503 MB. For comparison a run with $n = 10$, consumed only 21 seconds, the maximum memory being 800 kB and maximum swap 3 MB.

Finally, Eq. (3.6) implies that oscillations found for the three discrete time models exist also for a more realistic continuous time model, after averaging correctly over initial conditions. We see that the VACF, for the lattice Lorentz gas, is a non analytical function of time t (even so for all times t, excluding $t = n$, second and higher time derivatives of the VACF are equal to zero). Therefore asymptotic large t expansions, which assume a smooth analytical behavior of the VACF, might fail. For lattice systems it is therefore important to consider first the large and discrete n behavior of the VACF, and only then use Eq. (3.6) to find the solution for large and continuous time t. This approach is pursued in the following section which considers the TSLG model.

IV. TWO STATE LORENTZ GAS

The two state Lorentz gas (TSLG), considers a light particle in a random A-B alloy. It was discussed to some extent in subsection III A. The model defines a probability p, that a lattice site is occupied by a scatterer whose transmission coefficient is η and the probability $(1-p)$ for a scatterer whose transmission coefficient is $(\eta + \varepsilon)$. Since $\eta + \varepsilon \leqslant 1$ we obviously have $0 \leqslant \varepsilon \leqslant 1 - \eta$. The average transmission coefficient is

$$T = \eta + \varepsilon(1-p) \tag{4.1}$$

and the average reflection coefficient is $R = 1 - T$. Defining the local deviation from the mean value $\delta T_m \equiv T_m - T$, we shall use a perturbative expansion in the fluctuation δT_m, the zeroth order in this expansion being the ordered system. The statistical properties of δT_m are determined by $\langle \delta T_m \rangle = 0$,

$$\delta^2 \equiv \langle (\delta T_m)^2 \rangle = p(1-p)\,\varepsilon^2 \tag{4.2}$$

and

$$\langle (\delta T_m)^i \rangle = \varepsilon^i [(-1)^i p(1-p)^i + p^i (1-p)] \tag{4.3}$$

which is independent of η. Notice that $\delta^2 = 0$ for three cases, either $\varepsilon = 0$, or $p = 1$, or $p = 0$, all corresponding to ordered systems. For odd i and $p < 1/2$, $\langle (\delta T_m)^i \rangle \leqslant 0$, while for $p > 1/2$, $\langle (\delta T_m)^i \rangle \geqslant 0$.

To derive the perturbation expansion, we use the mathematical tools and results obtained in Section II, Eqs. (2.1)–(2.14). We rewrite Eq. (2.10) as

$$\begin{aligned} T_{qq'} &= T \delta_{qq'} + (\delta T)_{qq'} \\ R_{qq'} &= \delta_{qq'} - T_{qq'} \end{aligned} \tag{4.4}$$

where we use

$$(\delta T)_{qq'} \equiv \frac{1}{M} \sum_m e^{i(q-q')m} \delta T_m \tag{4.5}$$

We find it useful to separate L into two parts, $L \equiv L_0 + \Delta L$, with

$$\begin{aligned} (L_0^{++})_{qq'} &= [(L_0^{--})_{qq'}]^* = -T \delta_{qq'} e^{iq'} \\ (L_0^{+-})_{qq'} &= [(L_0^{-+})_{qq'}]^* = -R \delta_{qq'} e^{-iq'} \end{aligned} \tag{4.6}$$

$[\cdots]^*$ means the complex conjugate of $[\cdots]$, and

$$\begin{aligned} (\Delta L^{++})_{qq'} &= -(\delta T)_{qq'} e^{iq'} \\ (\Delta L^{+-})_{qq'} &= (\delta T)_{qq'} e^{-iq'} \\ (\Delta L^{-+})_{qq'} &= (\delta T)_{qq'} e^{iq'} \\ (\Delta L^{--})_{qq'} &= -(\delta T)_{qq'} e^{-iq'} \end{aligned} \tag{4.7}$$

Notice that if the system is ordered then $\delta T_m = 0$ and so $\Delta L = 0$.

We use the matrix identity

$$(z + L_0 + \Delta L)^{-1} = \sum_{k=0}^{\infty} (-1)^k l_0^{-1}(z) \times \Delta L \times l_0^{-1}(z) \cdots \Delta L \times l_0^{-1}(z) \tag{4.8}$$

where

$$l_0^{-1}(z) \equiv (z + L_0)^{-1} \tag{4.9}$$

The kth term in the sum Eq. (4.8) contains $k+1$ multipliers of type $l_0^{-1}(z)$ and k multipliers of type ΔL. Inserting the expansion Eq. (4.8) in the formal solution Eq. (2.14) the exact solution can be expressed as a power series

$$\langle \hat{P}_q(z) \rangle = \sum_{k=0}^{\infty} \langle \hat{P}_q(z) \rangle_k \tag{4.10}$$

with

$$\langle \hat{P}_q(z) \rangle_k = z(-1)^k \langle \hat{\lambda}^k(z)\, l_0^{-1}(z)\, P_q(0) \rangle \tag{4.11}$$

and

$$\hat{\lambda}(z) \equiv l_0^{-1} \times \Delta L \tag{4.12}$$

We shall assume that the initial conditions $P_q(0)$ and the static disorder (the random variables T_m) are statistically independent, so that

$$\langle \hat{P}_q(z) \rangle = \sum_{k=0}^{\infty} (-1)^k \langle \hat{\lambda}^k(z) \rangle \langle \hat{P}_q(z) \rangle_0 \tag{4.13}$$

An important ingredient of our solution is the $2M \times 2M$ matrix (Green function)

$$l_0^{-1}(z) = \begin{pmatrix} l_0^{-1}(z)^{++} & l_0^{-1}(z)^{+-} \\ l_0^{-1}(z)^{-+} & l_0^{-1}(z)^{-} \end{pmatrix} \tag{4.14}$$

given by

$$\begin{aligned} [l_0^{-1}(z)^{++}]_{qq'} &= [l_0^{-1}(z)^{--}]^*_{qq'} = \frac{(z - Te^{-iq})}{f(q,z)} \delta_{qq'} \\ [l_0^{-1}(z)^{+-}]_{qq'} &= [l_0^{-1}(z)^{-+}]^*_{qq'} = \frac{Re^{-iq}}{f(q,z)} \delta_{qq'} \end{aligned} \tag{4.15}$$

where

$$f(q,z) = z^2 - 2zT\cos q + T - R \tag{4.16}$$

Equation (4.15) can be verified easily by showing that $l_0^{-1}(z) \times (L_0 + z) = \delta_{qq'}$, with L_0 defined in Eq. (4.6).

An explicit expression for the propagator $\hat{\lambda}(z)$ is found using Eqs. (4.7), (4.9) and (4.15)

$$[\hat{\lambda}^{\alpha\beta}(z)]_{qq'} = -(\alpha\beta)\frac{z - e^{-\alpha iq}}{f(q,z)}\delta T_{qq'}\, e^{\beta iq} \tag{4.17}$$

Here α and β in the left hand side of the equation get the values $+$ or $-$, whereas in the right hand side they correspond to the values ± 1.

Below we shall investigate the VACF for the case when the light particle velocity is initially directed to the right, implying

$$P^{+}_{q=0}(0) = 1, \qquad P^{-}_{q=0}(0) = 0 \tag{4.18}$$

Then the VACF in z space is

$$\langle \hat{v}(z)\, v(0) \mid v(0) = +1 \rangle = \langle \hat{P}^{+}_{q=0}(z) \rangle - \langle \hat{P}^{-}_{q=0}(z) \rangle \tag{4.19}$$

Using our formal expansion:

$$\langle \hat{v}(z)\, v(0) \mid v(0) = +1 \rangle = \sum_{k=0}^{\infty} \langle \hat{v}(z)\, v(0) \mid v(0) = +1 \rangle_k \tag{4.20}$$

where

$$\langle \hat{v}(z)\, v(0) \mid v(0) = +1 \rangle_k = \langle \hat{P}^{+}_{q=0}(z) \rangle_k - \langle \hat{P}^{-}_{q=0}(z) \rangle_k \tag{4.21}$$

In a way similar to Eq. (4.20), expansions for the mean, mean square displacement and higher moments of the displacement or the velocity correlations can be written. However mainly the VACF will be considered below.

A. Ordered System

When the system is ordered the stochastic Lorentz model is an example of a persistent random walk,[35] meaning that the jump probabilities depend on the direction from which the particle has arrived. Even though this case is rather trivial, we derive the following results for the sake of completeness and in order to contrast between the ordered system and the disordered one. Equation (4.30) is our main result relevant to the rest of the work, it shows that for the ordered system the VACF decays exponentially with time.

When fluctuations are neglected (i.e., $\Delta L = 0$) we find

$$\langle \hat{P}^{+}_{q}(z) \rangle_0 = z\frac{P^{+}_{q}(0)(z - Te^{-iq}) + P^{-}_{q}(0)\, Re^{-iq}}{z^2 - 2Tz\cos q + T - R} \tag{4.22}$$

and

$$\langle \hat{P}_q^-(z)\rangle_0 = z\,\frac{P_q^+(0)\,Re^{iq} + P_q^-(0)(z - Te^{iq})}{z^2 - 2Tz\cos q + T - R} \tag{4.23}$$

It is possible to $z \to n$ transform Eqs. (4.22) and (4.23) using the inverse transform Eq. (2.7) to find

$$\begin{aligned}\langle P_q^+(n)\rangle_0 = &\frac{1}{2\sqrt{T^2\cos^2 q - (T-R)}}\\ &\times\{[z_+^n(z_+ - Te^{-iq}) - z_-^n(z_- Te^{-iq})]\,P_q^+(0)\\ &+ (z_+^n - z_-^n)\,Re^{-iq}P_q^-(0)\}\end{aligned} \tag{4.24}$$

and

$$\begin{aligned}\langle P_q^-(n)\rangle_0 = &\frac{1}{2\sqrt{T^2\cos^2 q - (T-R)}}\\ &\times\{(z_+^n - z_-^n)\,Re^{iq}P_q^+(0)\\ &+ [z_+^n(z_+ - Te^{iq}) - z^n{}_-(z_- Te^{iq})]\,P_q^-(0)\}\end{aligned} \tag{4.25}$$

with

$$z_\pm = T\cos q \pm \sqrt{T^2\cos^2 q - (T-R)} \tag{4.26}$$

From this solution the moments $\langle x^k(n)\rangle$ can be found in the usual way (i.e., by differentiating the solution k times with respect to q and then assigning $q = 0$). It is then easy to show that the diffusion coefficient is $D_0 = T/(2R)$, or in terms of the original parameters of the model

$$D_0 = \frac{\eta + (1-p)\,\varepsilon}{2[1 - \eta - (1-p)\,\varepsilon]} \tag{4.27}$$

The probability that the light particle has a velocity $\pm v$, at a time n, is $\langle P^{\pm}_{q=0}(n)\rangle_0$. From Eqs. (4.24) and (4.25),

$$\langle P^{\pm}_{q=0}(n)\rangle_0 = \tfrac{1}{2}\{[1 + (T-R)^n]\,P^{\pm}_{q=0}(0) + [1 - (T-R)^n]\,P^{\mp}_{q=0}(0)\} \tag{4.28}$$

For $n \to \infty$ and $T \neq 1$, $T \neq 0$ the equilibrium

$$\lim_{n\to\infty} \langle P^{+}_{q=0}(n)\rangle_0 = \lim_{n\to\infty} \langle P^{-}_{q=0}(n)\rangle_0 = \tfrac{1}{2} \tag{4.29}$$

is reached for any normalized initial condition .

The initial condition Eq. (4.18) are now chosen. Then the VACF is

$$\begin{aligned}\langle v(n)\, v(0) \mid v(0) = +1\rangle_0 &= \langle P^{+}_{q=0}(n)\rangle_0 - \langle P^{-}_{q=0}(n)\rangle_0 \\ &= \exp(-n/t_{Rel})\end{aligned} \tag{4.30}$$

with

$$t_{Rel} \equiv \left[\ln \frac{1}{T-R}\right]^{-1} \tag{4.31}$$

The relaxation time $t_{Rel} = 0$ when $T = R = 1/2$ meaning that after a single collision event there is a probability 1/2 to find the light particle with initial velocity is $+1$ with a velocity -1. That is why the instantaneous decay of the VACF is of no surprise. An oscillatory type of behavior is found when $T < 0.5$. When $T = 0$ and $R = 1$ initial conditions do not decay and the real part of the relaxation time is zero (pure oscillations). When $T = 1$ the relaxation time diverges as expected from a system with no reflection.

B. Lowest Order Contribution of Disorder

We shall now calculate the corrections to the zeroth order solution due to disorder. Since $\langle \Delta L\rangle = 0$, the $\langle \hat{P}_q(z)\rangle_1$ term appearing in Eq. (4.10), which has a linear dependence on ΔL, vanishes. We shall calculate the next term in our expansion

$$\langle \hat{P}_q(z)\rangle_2 = \langle \hat{\lambda}^2(z)\rangle \langle \hat{P}_q(z)\rangle_0 \tag{4.32}$$

For our calculation we use

$$\langle \delta T_m\, \delta T_j\rangle = \delta^2\, \delta_{mj} \tag{4.33}$$

where δ^2 is given in Eq. (4.2). In Fourier space Eq. (4.33) yields

$$\langle \delta T_{qq''}\, \delta T_{q''q'}\rangle = \frac{\delta^2}{M}\, \delta_{qq'} \tag{4.34}$$

as can be easily proven using Eqs. (2.5) and (2.6). After some algebra, and using Eqs. (4.16) and 4.17) we find

$$\begin{aligned}\langle \lambda^2(z)\rangle^{++} &= [\langle \lambda^2(z)\rangle^{--}]^* = \delta^2 \frac{z - e^{-iq}}{f(q,z)} \hat{h}(z)\, e^{iq}\, \delta_{qq'} \\ \langle \lambda^2(z)\rangle^{+-} &= [\langle \lambda^2(z)\rangle^{-+}]^* = -\delta^2 \frac{z - e^{-iq}}{f(q,z)} \hat{h}(z)\, e^{-iq}\, \delta_{qq'}\end{aligned} \tag{4.35}$$

where

$$\hat{h}(z) = \frac{1}{M} \sum_q \frac{2[z\cos q - 1]}{f(q,z)} \tag{4.36}$$

Using Eqs. (4.32) and (4.35) we have

$$\langle \hat{P}_q^+(z)\rangle_2 = \frac{\delta^2 \hat{h}(z)(z - e^{-iq})}{f(q,z)} [e^{iq}\langle \hat{P}_q^+(z)\rangle_0 - e^{-iq}\langle \hat{P}_q^-(z)\rangle_0] \tag{4.37}$$

with $\langle \hat{P}_q^{\pm}(z)\rangle_0$ given in Eqs. (4.22) and (4.23) and

$$\langle \hat{P}_q^-(z)\rangle_2 = \frac{\delta^2 \hat{h}(z)(z - e^{iq})}{f(q,z)} [-e^{iq}\langle \hat{P}_q^+(z)\rangle_0 + e^{-iq}\langle \hat{P}_q^-(z)\rangle_0] \tag{4.38}$$

It follows from Eqs. (4.37) and (4.38) that

$$\begin{aligned}&\langle \hat{P}_q^+(z)\rangle_2 + \langle \hat{P}_q^-(z)\rangle_2 \\ &\quad = \delta^2 2i \sin(q) \frac{\hat{h}(z)}{f(q,z)} [e^{iq}\langle \hat{P}_q^+(z)\rangle_0 - e^{-iq}\langle \hat{P}_q^-(z)\rangle_0]\end{aligned} \tag{4.39}$$

Equations (4.37)–(4.39) make our main results so far. Using them we will derive the δ^2 corrections to the VACF, Eq. (4.30). Notice that according to Eq. (4.39)

$$\langle \hat{P}^+_{q=0}(z)\rangle_2 + \langle \hat{P}^-_{q=0}(z)\rangle_2 = 0 \tag{4.40}$$

and the δ^2 correction terms do not alter the normalization condition.

The second order correction to the VACF, Eq. (4.30), in z space, is found using Eq. (4.21)

$$\langle \hat{v}(z)\, v(0) \mid v(0) = +1\rangle_2 = \frac{2\delta^2 z \hat{h}(z)}{(z - \Delta)^2} \tag{4.41}$$

where we have defined $\Delta \equiv T - R$. In the following two subsections we shall investigate the $z \to n$ transformation of this function in some detail, and compare this approximate solution with the exact solution found for $n \leqslant 20$.

1. Case $T = R$. We shall now consider the special case, $T = R = 1/2$, for which the exact $z \to n$ transformation, Eq. (2.7), of the VACF, Eq. (4.41), is

$$\langle v(n)\, v(0) \mid v(0) = +1 \rangle_2 = \delta^2 \frac{2}{i\pi} \oint \frac{1}{M} \sum_q \frac{z \cos q - 1}{z - \cos q} z^{n-3}\, dz \tag{4.42}$$

Changing the order of the integration and the summation in this equation we consider the thermodynamic limit, which means that we replace the sum $1/M \sum_q \cdots$ by the integral $(1/2\pi) \int_{-\pi}^{\pi} dq \cdots$. Some elementary integrations then give

$$\langle v(n)\, v(0) \mid v(0) = +1 \rangle_2 = \begin{cases} -4\delta^2 \dfrac{1}{2^{n-1}} \dbinom{n-1}{n-1/2} \dfrac{1}{n-2} & n \text{ is odd, } n \neq 1 \\ 0 & n \text{ is even} \end{cases} \tag{4.43}$$

and $\langle v(n=1)\, v(0) \mid v(0) = +1 \rangle_2 = 0$. Using the Stirling approximation

$$n! \simeq \left(\frac{n}{e}\right)^n \sqrt{2\pi n}$$

for $n \gg 1$ and odd

$$\langle v(n)\, v(0) \mid v(0) = +1 \rangle_2 \simeq -4\delta^2 \sqrt{\frac{2}{\pi}}\, n^{-3/2} \tag{4.44}$$

showing the power law decay of the type found for the space disordered Lorentz gas, Eq. (1.1).

We compare our result obtained here with the exact result obtained by the symbolic programming approach, for parameters $p = 1/2$, $\eta = 12/25$ and $\varepsilon = 1/25$. The exact result for this case has been presented already in Fig. 1 where one can observe a fairly good agreement between the asymptotic solution Eq. (4.44) (dashed line) and the exact solution for the times $10 < n < 20$. Figure 4 shows the ratio between the exact VACF and the approximate solution, Eq. (4.43), for $n < 20$ and odd. There is a very good

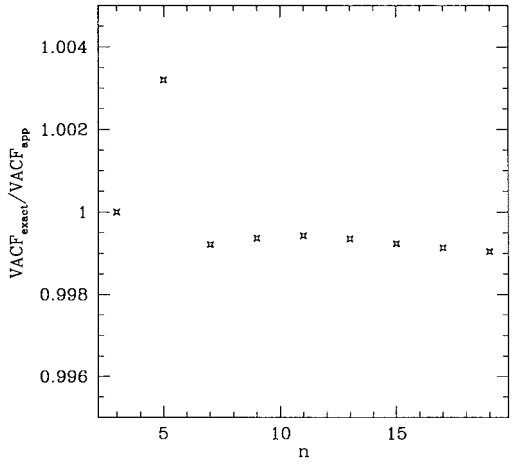

Fig. 4. Ratio of the exact VACF, Table 1, and the approximate solution obtained by means of the perturbation theory.

agreement between the approximate and exact results. For even n the perturbation theory gives a vanishing VACF, while the exact result shows that the VACF for even n is finite though very small compared to the VACF for odd n.

2. Case $T \neq R$. A more general case when the averaged transmission and reflection probabilities are not necessarily equal to one half is now considered. Taking the thermodynamic limit of Eq. (4.36) yields

$$\hat{h}(z) = \frac{1}{T}\left[-1 + \sqrt{\frac{1 - z^{-2}}{1 - \Delta^2 z^{-2}}} \right] \tag{4.45}$$

and using Eq. (4.41)

$$\langle \hat{v}(z)\, v(0) \mid v(0) = +1 \rangle_2 = \frac{2\delta^2}{T} \frac{z^{-1}}{(1 - \Delta z^{-1})^2} \left[-1 + \sqrt{\frac{1 - z^{-2}}{1 - \Delta^2 z^{-2}}} \right] \tag{4.46}$$

Now according to the definition of the discrete Laplace z transformation we have

$$\langle \hat{v}(z)\, v(0) \mid v(0) = +1 \rangle_2 = \sum_{n=0}^{\infty} z^{-n} \langle v(n)\, v(0) \mid v(0) = +1 \rangle_2 \tag{4.47}$$

To find the small n behavior of the VACF, Eq. (4.46) is expanded in powers of z^{-1} around $z^{-1}=0$. Then according to Eq. (4.47) the nth coefficient in this expansion gives $\langle v(n)\, v(0) \mid v(0)=+1\rangle_2$. For small n it is convenient to carry out the expansion using Mathematica[25] which produces

$$\begin{aligned}
&\frac{T}{2\delta^2}\langle \hat{v}(z)\, v(0) \mid v(0)=+1\rangle_2 \\
&\quad = (-1/2+\Delta^2/2)\, z^{-3} + (-\Delta+\Delta^3)\, z^{-4} \\
&\qquad + (-1/8-7\Delta^2/4+15\Delta^4/8)\, z^{-5} + (-\Delta/4-5\Delta^3/2+11\Delta^5/4)\, z^{-6} \\
&\qquad + (-1/16-7\Delta^2/16-55\Delta^4/16+63\Delta^6/16)\, z^{-7} \\
&\qquad + (-\Delta/8-5\Delta^3/8-35\Delta^5/8+41\Delta^7/8)\, z^{-8}\cdots
\end{aligned} \tag{4.48}$$

For different choices of $-1<\Delta<1$ and for $n\leqslant 1000$ we have found that carrying out such expansions using Mathematica on a standard computer[34] consumes a short time.

We have noticed [see Fig. 1] that the VACF decays as a power law with an *oscillating* amplitude, the period of oscillations being two time units. These fast oscillations are found when the large n behavior of the VACF is investigated. For this aim we have calculated the $z\to n$ transformation of Eq. (4.46) in the limit of large n. In Appendix B we find the large time behavior of the VACF, Eq. (4.46),

$$\langle v(n)\, v(0) \mid v(0)=+1\rangle_2 \sim \begin{cases} -\delta^2 \dfrac{1}{\sqrt{32\pi(TR)^5}} \dfrac{T-R}{T}\, n^{-3/2}, & \text{if } n \text{ is even} \\ -\delta^2 \dfrac{1}{\sqrt{32\pi(TR)^5}} \dfrac{T^2+R^2}{T}\, n^{-3/2}, & \text{if } n \text{ is odd} \end{cases} \tag{4.49}$$

The characteristic 3/2 power law decay of the VACF, Eq. (1.1), found previously for the space disordered system is found here for $TR\neq 0$. However now oscillations are also found. As shown in Appendix B the asymptotic behavior is expected to hold only for large times, n, satisfying

$$-n\ln(|T-R|)\gg 1 \tag{4.50}$$

If $T\to 1$ or $R\to 1$ these times are especially long.

Figure 5 compares: (i) our exact results for the VACF presented in Table 1, (ii) the perturbation theory result found using Eqs. (4.30), (4.47) and (4.48), and (iii) the asymptotic result, Eq. (4.49). We use $\eta = 0.5$, $p = 0.5$ and $\varepsilon = 0.1$ and consider the time window $0 \leqslant n \leqslant 20$. This choice of parameters implies that $T = 0.55$ and $\delta^2 = 1/400$. Due to a good agreement between the approximate and the exact results the approximate values of the VACF presented in Fig. 5 cannot be distinguished from the exact ones. A closer look at the numerical data shows that deviations exist between the exact and perturbation results. For odd n the average ratio (exact VACF/perturbative VACF) is 0.994 while for even n this ratio is 0.942.

In Fig. 5 one can also see that already after fifteen collisions the asymptotic results converge to the exact ones. For $n \geqslant 10$ we have fitted[25] the exact results for the VACF with an $n^{-3/2}$ behavior. For odd n we find $\langle v(n)\, v(0) \mid v(0) = +1 \rangle \simeq -0.00774 n^{-3/2}$ while for even n we find $\langle v(n)\, v(0) \mid v(0) = +1 \rangle \simeq -0.00195 n^{-3/2}$. These fittings are expected to work well when $n \to \infty$. They are compared with the asymptotic behavior of the VACF calculated using the perturbation theory. Using Eq. (4.49), we find for odd n, $\langle v(n)\, v(0) \mid v(0) = +1 \rangle \sim -0.00751 n^{-3/2}$ and for even n, $\langle v(n)\, v(0) \mid v(0) = +1 \rangle \sim -0.00149 n^{-3/2}$. Thus for odd n the two results are in fairly good agreement even though $10 \leqslant n \leqslant 20$. For larger n we expect to find an even better fit between the exact results and the asymptotic $n^{-3/2}$ behavior, Eq. (4.49).

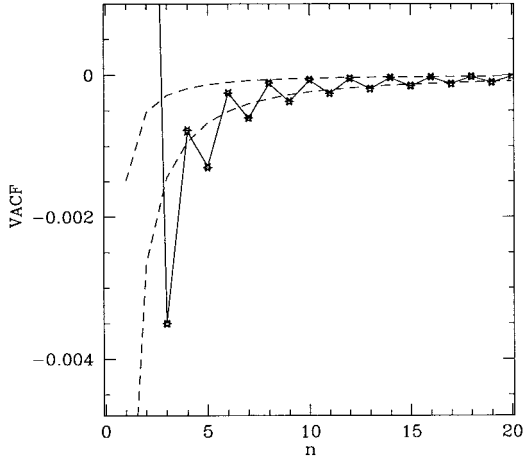

Fig. 5. Time dependence of the exact result $\langle v(n)\, v(0) \mid v(0) = +1 \rangle$, perturbation theory result $\langle v(n)\, v(0) \mid v(0) = +1 \rangle_0 + \langle v(n)\, v(0) \mid v(0) = +1 \rangle_2$, and asymptotic expressions (dashed curves) Eq. (4.49).

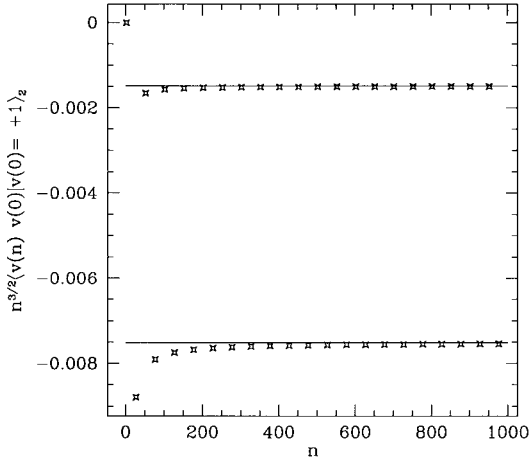

Fig. 6. Plot of $n^{3/2}\langle v(n)\, v(0) \mid v(0) = +1\rangle_2$ vs n for the parameters: $\eta = 0.5$, $p = 0.5$ and $\varepsilon = 0.1$. The straight curves are the asymptotic results Eq. (4.49).

Figures 6 and 7 show $n^{3/2}\langle v(n)\, v(0) \mid v(0) = +1\rangle_2$ vs n. These figures demonstrate how $\langle v(n)\, v(0) \mid v(0) = +1\rangle_2$ converges to its asymptotic behavior, Eq. (4.49). To obtain $n^{3/2}\langle v(n)\, v(0) \mid v(0) = +1\rangle_2$ we have expanded $\langle \hat{v}(z)\, v(0) \mid v(0) = +1\rangle_2$ in powers of z^{-1} as was done in Eq. (4.48). Also shown in the two figures are the asymptotic results for odd and even n, Eq. (4.49). In Fig. 6 where $T = 0.55$ one sees a swift convergence of the values obtained by the series expansion to the asymptotic result for $n \leqslant 1000$. In Fig. 7 we choose $T = 0.925$ and there the convergence to the

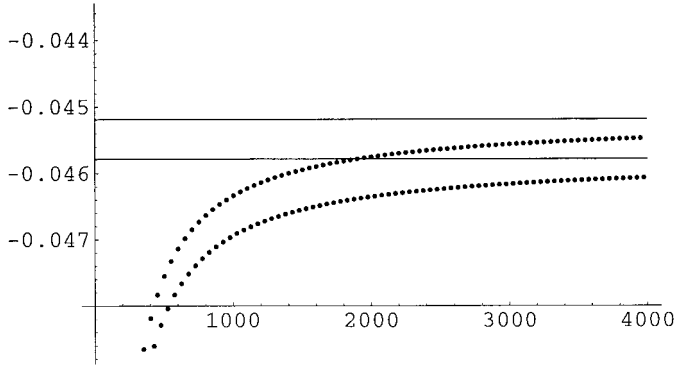

Fig. 7. The same as Fig. 6 with parameters $\eta = 0.9$, $p = 0.5$ and $\varepsilon = 0.05$, meaning $T = 0.925$. Notice that the convergence of the small n expansion to the asymptotic result is slower than that shown in Fig. 6.

asymptotic behavior is much slower. This slow convergence is expected when either $T \to 1$ or $R \to 1$.

The oscillations found in Eq. (4.49) are very fast since their period is only twice the shortest time scale of the problem (i.e., the flight time from one lattice point to its nearest neighbor). An interesting quantity is the coarse grained VACF defined

$$\overline{\langle v(n+1/2)\, v(0) \mid v(0) = +1 \rangle_2}$$

$$= \frac{1}{2} [\langle v(n+1)\, v(0) \mid v(0) = +1 \rangle_2 + \langle v(n)\, v(0) \mid v(0) = +1 \rangle_2]$$

$$\sim -\delta^2 \frac{1}{4R\sqrt{2\pi(TR)^3}}\, n^{-3/2} \tag{4.51}$$

The VACF fluctuates around this averaged value. In terms of the original parameters of the problem

$$\overline{\langle v(n+1/2)\, v(0) \mid v(0) = +1 \rangle_2}$$

$$\sim -\varepsilon^2 p(1-p) \frac{1}{4\sqrt{2\pi}} \{[\eta + \varepsilon(1-p)]^3\, [1 - \eta - \varepsilon(1-p)]^5\}^{-1/2}\, n^{-3/2} \tag{4.52}$$

It is easy to see that when

$$\eta \gg \varepsilon(1-p) \qquad \text{and} \qquad 1 - \eta \gg \varepsilon(1-p) \tag{4.53}$$

$$\overline{\langle v(n+1/2)\, v(0) \mid v(0) = +1 \rangle_2}$$

$$\sim -\varepsilon^2 p(1-p) \frac{1}{4\sqrt{2\pi}} [\eta^3 (1-\eta)^5]^{-3/2}\, n^{-3/2} + o(\varepsilon^3) \tag{4.54}$$

This equation shows a quadratic dependence of the VACF on the small parameter ε. However, when $\eta \to 0$ or $\eta \to 1$ Eq. (4.54) is not valid and a more careful investigation of the small ε behavior of the VACF is needed.

We define $\eta = 1 - B_1 \varepsilon$ and find from the condition $0 \leqslant \eta + \varepsilon \leqslant 1$ that $1 \leqslant B_1 \leqslant 1/\varepsilon$. For this representation of parameters $T = 1 - \varepsilon(B_1 - 1 + p)$. Then when $\varepsilon(B_1 - 1 + p) \ll 1$ (the system is nearly transparent) we find

$$\overline{\langle v(n+1/2)\, v(0) \mid v(0) = +1 \rangle_2}$$

$$\sim -\varepsilon^{-1/2} p(1-p) \times \frac{1}{4\sqrt{2\pi}} (B_1 - 1 + p)^{-5/2}\, n^{-3/2} \tag{4.55}$$

We see that the VACF diverges as $\varepsilon \to 0$ (we assume $p \simeq 1/2$) and our expansion is not valid for this case.

In a similar way we define $\eta = B_0 \varepsilon$ and from the condition $0 \leqslant \eta + \varepsilon \leqslant 1$ we find $0 \leqslant B_0 \leqslant 1/\varepsilon - 1$. The transmission coefficient is now $T = \varepsilon(B_0 + 1 - p)$ and for small B_0 and ε the system is nearly reflecting. We assume $\varepsilon(B_0 + 1 - p) \ll 1$ and then find that

$$\overline{\langle v(n+1/2)\, v(0) \mid v(0) = +1 \rangle}_2$$

$$\sim -\varepsilon^{1/2} p(1-p) \times \frac{1}{4\sqrt{2\pi}} (B_0 + 1 - p)^{-3/2} n^{-3/2} \tag{4.56}$$

For this case the second order corrections to the VACF is non-diverging.

V. SUMMARY AND DISCUSSION

We have used a symbolic programming approach to find exact results for the one-dimensional Lorentz gas on a lattice for the case when the transmission coefficients $\{T_m\}$ are independent identically distributed random variables. It is quite practical to compute this exact solution for times $n \leqslant 20$. When all lattice points are occupied by scatterers this means that each particle has encountered twenty collisions. When collisions are strong twenty collisions are sufficient to reduce the VACF by a few orders of magnitudes.

We have found for three models of disorder (i.e., TSLG, space and uniform disorders) characteristic fast oscillations of the VACF. These oscillations are due to the fact that the scatterers are placed on a lattice. Our main concern was lattice Lorentz gas were both space and time are discrete (this enables a relatively simple solution in terms of the Mathematica program). We showed in Eq. (3.6), how to use the discrete solution to obtain the VACF for continuous time where the light particle is initially located randomly on the real line (i.e., not necessarily on a lattice point). Averaging over this more realistic initial condition we still find an oscillating VACF which is not a smooth function of time.

For the TSLG model (random A-B alloy) we have found a good agreement between exact results and those computed by the ε perturbation theory. For the case of n even and $T = R$ the second order perturbation theory gives a VACF which equals zero, while the exact result shows that the VACF is finite though small compared to its values for odd n. For some choices of parameters, symbolic programming can be used to begin and explore the asymptotic long time behavior of the lattice Lorentz gas.

Using the perturbation theory we have found that the TSLG exhibits a 3/2 power decay. The discrete time perturbation theory exhibits two different types of 3/2 decay the first for n odd and the second for n even [as predicted in Eq. (4.49)]. After finding the large n discrete time solution for even and odd n one may investigate the large continuous t behavior of an ensemble of light particles distributed at time $t=0$ randomly on the real line. This is done simply by connecting (with a straight line) the values of the discrete VACF for $\mathrm{Int}(t)$ and $\mathrm{Int}(t)+1$ (i.e., the VACF, for lattice systems is a non-analytical function of time, even after averaging over equilibrium initial conditions). As a consequence asymptotic large t expansions of the VACF for continuous time t, which assume a smooth analytical behavior of the VACF for large times in the first place, might lead to wrong conclusions. Such a non analytical behavior is not expected to be found for scatterers distributed randomly on the real line, the random intervals between them described by an exponential distribution.

In our perturbation expansion, ε is a small parameter. One could have considered other parameters as being small [e.g., p or $(1-p)$]. However we realize that such density expansions are very different from ours.[13] To see this consider the fluctuation δT_m around the average transmission coefficient. In our expansion we have neglected terms of the order $\langle(\delta T_m)^i\rangle$ with $i>2$. According to Eq. (4.3) for small ε, $\langle(\delta T_m)^i\rangle \sim \varepsilon^i$ while for small p, $\langle(\delta T_m)^i\rangle \sim p$ Hence for our ε expansion it is reasonable to neglect the $\langle(\delta T_m)^i\rangle$ with $i>2$ corrections provided that ε is small. For a similar expansion in p one will have to sum an infinite number of terms to collect all the linear in p terms. In this sense the p expansion and the ε expansion are very different and here we have considered simpler case.

As mentioned, in this work we have analyzed with detail the odd/even oscillations. One should remember that another type of slower oscillations can also be observed. These oscillations are predicted already within the mean field approximation Eq. (4.30).

Using our exact results we have compared between the dynamics of the light particle in different types of disorder. We have shown that when the transmission coefficients T_m are independent identically distributed random variables the information contained within the first three moments of T_m is not sufficient to determine the VACF beyond the time $n=6$. When comparing between two models of quenched disorder (i.e., the TSLG and the uniform disorder models) we saw large deviations between the two models, for $6<n\leqslant 20$, even though $\langle T_m\rangle$, $\langle T_m^2\rangle$ and $\langle T_m^3\rangle$, were chosen identical for both models (in this case the uniform model exhibits a much slower decay of the VACF than the TSLG model). Hence there is a need for information on higher order moments, to determine correctly the long time behavior of the VACF.

We have used a CTRW argument to predict a sub diffusive behavior for the Lorentz gas model with a uniform distribution of transmission coefficients. More rigorous methods are needed to determine if such an anomalous behavior describes correctly the transport properties of the light particle.

Finally, we believe that symbolic programming can be used to investigate other interesting dynamics on quenched disorder. For example the lattice Lorentz gas in dimensions higher than one or the discrete time random walk in a random environment.

APPENDIX A. SYMBOLIC PROGRAM

The Mathematica program generates the VACF for ten time steps. The generalization to longer times is straightforward.

```
c
c Initial conditions and input data are set:
c
n = 10
l = n + 2
pp[ 0, 0 ] = 1
Do[ pp[ 0, m ] = 0, { m, 1, l } ]
Do[ pp[ 0, m ] = 0, { m, -l, -1 } ]
Do[ pm[ 0, m ] = 0, { m, -l, l } ]
c
c Solve recursion relations for arbitrary disorder
c
Do[
{ pp[ i, m ] = pp[ i-1, m-1 ] t[ m ] + pm[ i-1, m+1 ](1-t[ m ]),
pm[ i, m ] = pp[ i-1, m-1 ](1-t[ m ]) + pm[ i-1, m+1 ] t[ m ],
pp[ i, l ] = 0,
pp[ i, -l ] = 0,
pm[ i, l ] = 0,
pm[ i, -l ] = 0 },
{ i, 1, l },
{ m, -l+1, l-1 } ]
c
c The VACF
c
Do[ va[ i ] = Sum[ pp[ i, m ] - pm[ i, m ], { m, -l, l } ], { i, 1, n } ]
c
c Average over disorder
```

```
c
Do[ vaEx[ i] = Expand[ va[ i]], { i, n} ]
Do[ u[ i] = vaEx[ i]/.{ x_^5 - > T[5], x_^4 - > T[4],
   x_^3 - > T[3], x_^2 - > T[2]}, { i, 1, n} ]
Do[ t[ m] = T[1], { m, -n, n} ]
c
c The output, the average VACF
c
Do[ Write[ "VACF.exact", u[ i], i], { i, 1, n} ]
```

APPENDIX B. ASYMPTOTIC BEHAVIOR OF VACF

It is our aim here to find the $z \to n$ transformation of Eq. (4.46) in the limit of large n. First we consider the first term in the right hand side of Eq. (4.46). The term

$$Z^{-1}[z^{-1}/(1-\Delta z^{-1})^2] = n\Delta^{n-1}$$

(Z^{-1} is the inverse z transform) is neglected since for long times it is much smaller than the contribution of the second term in Eq. (4.46) (the term with the square root) which as we show now decays as a power of n.

To convert the VACF we use the Fourier integral {see Eq. (37.8) p. 161 in ref. 27}

$$\langle v(n)\, v(0) \mid v(0) = +1 \rangle_2 = \frac{1}{2\pi} \int_{-\pi}^{\pi} \langle \hat{v}(z = re^{i\phi})\, v(0) \mid v(0) = +1 \rangle_2\, r^n e^{in\phi}\, d\phi \tag{B.1}$$

here $r > R$ with R being the radius of a circle which encloses all the singularities of the function $\langle \hat{v}(z)\, v(0) \mid v(0) = +1 \rangle_2$. A simple analysis of the singularities shows that $r > 1$. Using Eqs. (4.46) and (B.1)

$$\langle v(n)\, v(0) \mid v(0) = +1 \rangle_2 = \frac{2\delta^2}{\pi T} Re \left[\int_0^{\pi} \frac{1/re^{-i\phi}}{(1-\Delta/re^{-i\phi})^2} \sqrt{\frac{1-1/r^2e^{-2i\phi}}{1-\Delta^2/r^2e^{-2i\phi}}}\, r^n e^{in\phi}\, d\phi \right] \tag{B.2}$$

We define $1/r \equiv \exp(-\mu)$ with μ being real, positive and small. Then we change the integration variable ϕ to $\xi = \phi - i\mu$ and find

$$\langle v(n)\, v(0) \mid v(0) = +1 \rangle_2 = \frac{2\delta^2}{\pi T} Re \left[\int_{-i\mu}^{\pi - i\mu} \frac{e^{-i\xi}}{(1-\Delta e^{-i\xi})^2} \sqrt{\frac{1-e^{-2i\xi}}{1-\Delta^2 e^{-2i\xi}}}\, e^{in\xi}\, d\xi \right] \tag{B.3}$$

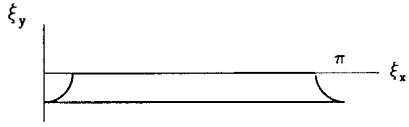

Fig. 8. The integration contour which helps to demonstrate the equivalence of Eq. (B.3) and Eq. (B.4). The arcs around $(0, 0)$ and $(0, \pi)$ have a radius $\mu \to 0$.

We now close the integration path, as shown in Fig. 8, along the real and positive axis in the ξ plane excluding the branching points at $\xi = 0$ and $\xi = \pi$. The contributions from the integrations along the arcs around the branching points [see Fig. 9] are negligible in the limit $\mu \to 0$. We therefore have

$$\langle v(n)\, v(0) \mid v(0) = +1 \rangle_2 = -\frac{2\delta^2}{\pi T} Re \left[\int_{\mu}^{\pi-\mu} F(\xi)\, e^{in\xi}\, d\xi \right] \tag{B.4}$$

with $\mu \to 0^+$ and

$$F(\xi) = \frac{e^{-i\xi}}{(1 - \Delta e^{-i\xi})^2} \sqrt{\frac{1 - e^{-2i\xi}}{1 - \Delta^2 e^{-2i\xi}}} \tag{B.5}$$

We now consider the integral

$$C = \oint F(\xi)\, e^{in\xi}\, d\xi \tag{B.6}$$

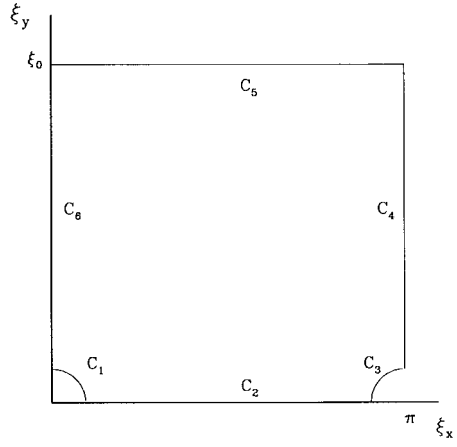

Fig. 9. The integration contour in the ξ plane along which the integral Eq. (B.6) is calculated. The arcs C_1 and C_3 have radius μ.

along the contour shown in Fig. 9. The integration path is chosen in such a way that all singular points are outside the contour meaning that ξ_0 defined in Fig. 9 satisfies the condition $\xi_0 < -\ln|\Delta|$ and hence $C=0$. As can be seen from Fig. 9

$$C = \sum_{i=1}^{6} C_i \tag{B.7}$$

with

$$\begin{aligned}
C_1 &= i\int_{\pi/2}^{0} F(\mu e^{i\theta}) \exp(in\mu e^{i\theta})\, \mu e^{i\theta}\, d\theta \\
\left(\frac{2\delta^2}{\pi T}\right) Re[C_2] &= -\langle v(n)\, v(0) \mid v(0) = +1\rangle_2 \\
C_3 &= i\int_{\pi}^{\pi/2} F(\pi + \mu e^{i\theta}) \exp(in\mu e^{in\theta})\, \mu e^{i\theta}\, d\theta \\
C_4 &= i\int_{\mu}^{\xi_0} F(\pi + iy)\, e^{in(\pi + iy)}\, dy \\
C_5 &= \int_{\pi}^{0} F(x + i\xi_0)\, e^{in(x + i\xi_0)}\, dx \\
C_6 &= i\int_{\xi_0}^{\mu} F(iy)\, e^{-ny}\, dy
\end{aligned} \tag{B.8}$$

It is easy to show that $\lim_{\mu\to 0} C_1 = \lim_{\mu\to 0} C_3 = 0$. When $n\to\infty$ the term C_5 gives only an exponentially small contribution of the order of $e^{-n\xi_0}$ and hence for large times can be neglected. The condition for such an approximation to be valid is $\xi_0 n \gg 1$ from which we find Eq. (4.50).

The integrals are calculated using

$$\begin{aligned}
C_4 &= i\int_{\mu}^{\xi_0} \frac{e^{-i(\pi + iy)}}{[1 - \Delta e^{-i(\pi + iy)}]^2} \sqrt{\frac{e^{-2i\pi} - e^{-2i(\pi + iy)}}{1 - \Delta^2 e^{-2i(\pi + iy)}}}\, e^{in(\pi + iy)}\, dy \\
&\sim \frac{-e^{i\pi n}}{(1+\Delta)^2 (1-\Delta^2)^{1/2}}\, n^{-3/2} \int_{n\mu}^{n\xi_0} \sqrt{2x}\, e^{-x}\, dx
\end{aligned} \tag{B.9}$$

We continue with our approximation and take the lower limit in the integral to be zero and the upper limit to infinity, then

$$C_4 \sim -\frac{e^{i\pi n}\sqrt{2}\,\Gamma(3/2)}{(1+\Delta)^2\,(1-\Delta^2)^{1/2}}\,n^{-3/2} \tag{B.10}$$

Using the same considerations

$$C_6 \sim \frac{\sqrt{2}\,\Gamma(3/2)}{(1-\Delta)^2\,(1-\Delta^2)^{1/2}}\,n^{-3/2} \tag{B.11}$$

We now use Eqs. (B.7) and (B.8) and the identities

$$\frac{1+\Delta^2}{(1-\Delta^2)^{5/2}} = \frac{2(T^2+R^2)}{(4RT)^{5/2}}$$

and

$$\frac{2\Delta}{(1-\Delta^2)^{5/2}} = \frac{2(T-R)}{(4RT)^{5/2}}$$

to find Eq. (4.49).

REFERENCES

1. M. H. Ernst and A. Weyland, *Phys. Lett.* **34A**:39 (1971).
2. L. A. Bunimovich and Ya. G. Sinai, *Commun. Math. Phys.* **78**:479 (1981).
3. H. van Beijeren, *Rev. Mod. Phys.* **54**:195 (1982).
4. J. Machta and R. Zwanzig, *Phys. Rev. Let.* **50**:1959 (1983).
5. J. P. Bouchaud and P. Le Doussal, *J. of Stat. Phys.* **41**:225 (1985).
6. A. Zacharel, T. Geisel, J. Nierwetberg, and G. Radons, *Phys. Let. A.* **114**:315 (1986).
7. P. Gaspard and G. Nicolis, *Phys. Rev. Let.* **65**:1693 (1990).
8. P. M. Bleher, *J. of Stat. Phys.* **66**:315 (1992).
9. H. van Beijeren and J. R. Dorfman, *Phys. Rev. Let.* **74**:4412 (1995).
10. Matsuoka and R. F. Martin, *J. of Stat. Phys.* **88**:81 (1997).
11. P. Levitz, *Europhys. Lett.* **39**:593 (1997).
12. E. Barkai, V. Fleurov, and J. Klafter (1998), submitted.
13. P. Grassberger, *Physica A* **103**:558 (1980).
14. H. van Beijeren and H. Spohn, *J. Stat. Phys.* **31**:231 (1983).
15. C. Olesky, *J. Phys. A. Math. Gen.* **23**:1275 (1990).
16. P. M. Binder and D. Frenkel, *Phys. Rev. A.* **42**:2463 (1990).
17. C. B. Briozzo, C. E. Budde, and M. O. Caceres, *Physica A.* **160**:225 (1989).
18. J. M. F. Gunn and M. Ortuño, *J. Phys. A. Math.* **18**:1095 (1985).
19. M. H. Ernst and G. A. van Velzen, *J. Stat. Phys.* **57**:455 (1989).
20. H. van Beijeren and M. H. Ernst, *J. Stat. Phys.* **70**:793 (1993).
21. E. G. D. Cohen and F. Wang, *J. Stat. Phys.* **81**:445 (1995).

22. F. Wang and E. G. D. Cohen, *J. Stat. Phys.* **81**:467 (1995).
23. M. H. Ernst, J. R. Dorfman, R. Nix, and D. Jacobs, *Phys. Rev. Let.* **74**:4416 (1995).
24. C. Apert, C. Bokel, J. R. Dorfman, and M. H. Ernst, *Physica D* **103**:357 (1997).
25. S. Wolfram, *Mathematica A System for Doing Mathematics by Computer* (Addison–Wesley Publishing Company, Inc., New York, Amsterdam, Tokyo 1988).
26. J. W. Haus and K. W. Kehr, *Physics Report* **150**:263 (1987).
27. G. Doetch, *Guide to the Applications of the Laplace and Z transforms* (Van Nostrand Reinhold Company, London, 1971).
28. R. Zwanzig, *J. Stat. Phys.* **28**:127 (1982).
29. P. J. H. Denteneer and M. H. Ernst, *Phys. Rev. B* **29**:1755 (1984).
30. H. Scher and M. Lax, *Phys. Rev. B* **7**:4491 (1973).
31. H. Scher and M. Lax, *Phys. Rev. B* **7**:4502 (1973).
32. H. Scher and E. W. Montroll, *Phys. Rev. B* **12**:2455 (1975).
33. G. H. Weiss, *Aspects and Applications of the Random Walk* (North Holland, Amsterdam, 1994).
34. http://www.tau.ac.il:81/cc/
35. J. W. Haus and K. W. Kehr, *J. Phys. Chem. Solids* **40**:1019 (1979).